

Article

Riverbed Micromorphology of the Yangtze River Estuary, China

Shuaihu Wu ^{1,2}, Heqin Cheng ^{1,*}, Y. Jun Xu ², Jiufa Li ¹, Shuwei Zheng ¹ and Wei Xu ¹

¹ State Key Lab of Estuarine & Coastal Research, East China Normal University, Shanghai 200062, China; wushuaihuxiaolaoda@163.com (S.W.); liover@online.sh.cn (J.L.); 798283317@qq.com (S.Z.); 2441162887@qq.com (W.X.)

² School of Renewable Natural Resources, Louisiana State University Agricultural Center, 227 Highland Road, Baton Rouge, LA 70803, USA; yjxu@lsu.edu

* Correspondence: hqch@sklec.ecnu.edu.cn; Tel.: +86-21-6254-6441

Academic Editor: Miklas Scholz

Received: 6 March 2016; Accepted: 18 April 2016; Published: 6 May 2016

Abstract: Dunes are present in nearly all fluvial channels and are vital in understanding sediment transport, deposition, and flow conditions during floods of rivers and estuaries. This information is pertinent for helping developing management practices to reduce risks in river transportation and engineering. Although a few recent studies have investigated the micromorphology of a portion of the Yangtze River estuary in China, our understanding of dune development in this large estuary is incomplete. It is also poorly understood how the development and characteristics of these dunes have been associated with human activities in the upper reach of the Yangtze River and two large-scale engineering projects in the estuarine zone. This study analyzed the feature in micromorphology of the entire Yangtze River estuary bed over the past three years and assessed the morphological response of the dunes to recent human activities. In 2012, 2014, and 2015, multi-beam bathymetric measurements were conducted on the channel surface of the Yangtze River estuary. The images were analyzed to characterize the subaqueous dunes and detect their changes over time. Bottom sediment samples were collected for grain size analysis to assess the physical properties of the dunes. We found that dunes in the Yangtze River estuary can be classified in four major classes: very large dunes, large dunes, medium dunes, and small dunes. Large dunes were predominant, amounting to 51.5%. There was a large area of dunes developed in the middle and upper reaches of the Yangtze River estuary and in the Hengsha Passage. A small area of dunes was observed for the first time in the turbidity maximum zone of the Yangtze River estuary. These dunes varied from 0.12 to 3.12 m in height with a wide range of wavelength from 2.83 to 127.89 m, yielding a range in height to wavelength of 0.003–0.136. Sharp leeside slope angles suggest that the steep slopes of asymmetrical dunes in the middle and upper reaches, and the turbidity maximum zone of the Yangtze River estuary face predominantly towards tides because of the ebb-dominated currents. Sharp windward slope angles in the lower reach of the North Passage show the influence of flood-dominated currents on dunes. It is likely that the scale of dunes will increase in the future in the South Channel because of a sharp decline of sediment discharge caused by recent human activities.

Keywords: channel morphology; river bedforms; multi-beam profiling; Yangtze River Estuary

1. Introduction

Subaqueous dunes are bedforms produced in river channels, estuaries, and coastal zones [1–3]. They are formed with different sediment sizes, mostly ranging from medium sand to gravel [4], and show rhythmic patterns caused by the interaction of turbulent flow on the riverbed [5]. The geometry of these dunes is a function of flow velocity, flow depth, and other physical parameters describing

sediments [6]. The length of dunes, measured by the distance between two consecutive crests, is generally approximately 10 times the height of the dunes, while the height is in the order of 10% to 30% of the flow depth [7]. Since dunes can significantly influence both the laminar and turbulent flow structure and can exert a strong control on the entrainment, transport, and deposition of sediment [8], the morphology and dynamics of dunes have been the nucleus of many scientific enquiries [9–12].

The study of dune development and dynamic evolution has been especially pertinent to river hydraulics and engineering [13–15]. Dunes may represent a hazard to pipelines [16]; their directional shift can have a significant impact on pipelines, as well as navigational channels, cables, and windmill turbines [17]. Depending on the scale of their dimension and migration rate, dunes have the potential to decrease navigable depths, thus making frequent dredging activities necessary [18]. Riverbank erosion, often driven by within-channel aggradation that is linked to the growth of dunes, can lead to significant population displacement and loss of infrastructure and agricultural land [19]. For instance, a subterranean tunnel was built in the Parana River (Argentina) in 1968; in 1983, large, long-lasting flood led to the formation of large dunes, which caused temporary exposure of the tunnel to flow over a distance of 250 m, thus threatening its stability [13]. The prediction of dune geometry is an essential component for estimating flow resistance and water levels during floods in rivers [20]. The form resistance due to dunes caused by local flow separation and recirculation can be significant and is dependent on their dimensions [20]. Consequently, many studies have been conducted on their classification and geometries [21–24].

A general concept for bedform evolution establishes that the sediment transport is the predominant contribution to dune formation. The concept has been applied in fluvial morphology for many decades [13]. In China, the Yangtze River discharges a large amount of sediment annually to the river's estuarine zone in different forms of motion (Figure 1), creating various subaqueous dunes in different forms and scales [25]. The Yangtze River Delta is one of the most industrialized areas in China and the river's mouth is one of the most important river transportation hubs in the world. Therefore, understanding of subaqueous dunes in the Yangtze River estuary can be crucial for helping maintain navigation safety, energy infrastructure, and civil and industrial assets. Although several studies on the estuarine riverbed dunes have been conducted [26–28], an inventory of the entire estuary is still incomplete. These studies mainly focused on the dunes in the South Channel and South Branch, and little is known for other parts of the large Yangtze River estuary, such as the important North Channel and Hengsha Passage. Especially, the studies focused on the dunes developed in the turbidity maximum zone are rare.

The Yangtze River Basin is one of the world's most populated river basins. With the increasing human interventions in the drainage basin and the estuary, implementations of many large-scale engineering within the river basin, e.g., the construction of the Three Gorge Dam (TGD) in the middle reach of the Yangtze River, have changed flow conditions in the river's lower reach and estuary [29]. Additionally, many river engineering practices in the Yangtze River estuary, e.g., channel deepening, and levee and port construction, have greatly changed the morphology and topography of the river main and distributary channels. The Yangtze estuarine Deeping Waterway project and the Qingcaosha Reservoir project may have especially affected the morphology of the Yangtze River estuary bottom. This study aimed to assess the changes of these channel beds using high-resolution bedforms, bathymetric charts, and sea-bottom sediment, as well as discharge and sediment load data. The primary goal was to document current development and morphological characteristics of dunes in the Yangtze River estuary and to explore the morphological response of dunes to the human activities. This work will enrich the study of dunes and provide important data for river channel morphology research.

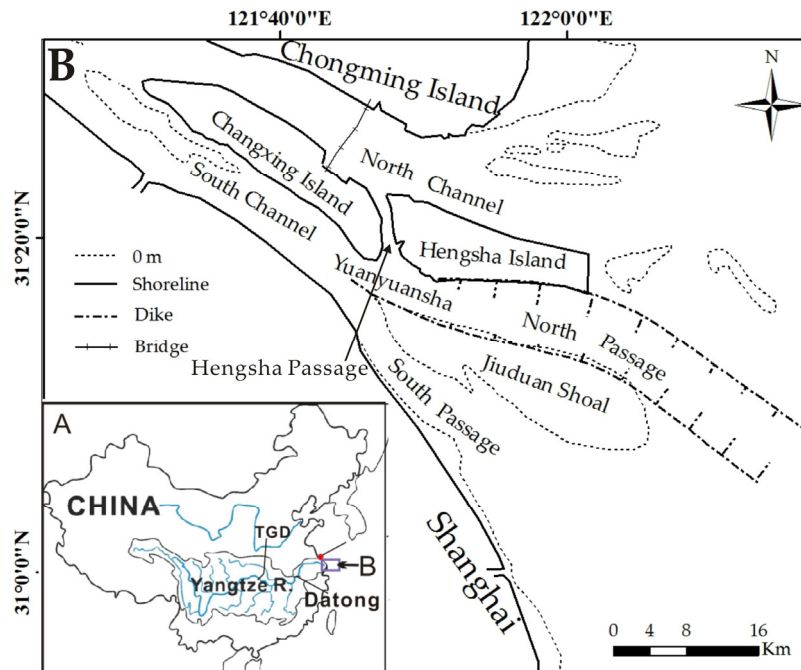


Figure 1. Geographical location of the study area—the Yangtze River estuary in China, with the Changxing Island, Hengsha Island, the North and South Channels and Passages, and the Jiuduansha Shoal wetland.

2. Methods

2.1. Study Area

Draining a land area of approximately 1.8 million km², the Yangtze River is the fourth largest river in terms of sediment load in the world [30–32]. The Yangtze River estuary is commonly considered as the 700 km long lowest reach of the Yangtze River that enters the East China Sea. The last 120 km estuarine section from Xuliujing to the following part presents a “three-order bifurcation and four outlets into the sea” pattern, which is divided first into the North and the South Branches by the Chongming Island (Figure 1). The South Branch is further divided into the North and the South Channels by the Changxing Island and the Hengsha Island. The South Channel is, again, further divided by the Jiuduansha wetland into the North Passage and the South Passage. The mouth bar section is geographically located between E 121°45′–122°30′ and N 30°45′–31°45′. The turbidity maximum exists in the river mouth-bar area all year round, has high suspended particle material content in the waters due to the interaction of freshwater and tidal flows, and could extend to the 10 m isobath in the flood season [33].

The multiyear averaged discharge was 29,300 m³/s at the Datong Hydrological Gauging Station, about 640 km up-estuary from the river mouth [34]. The runoff has obvious change with seasons, commonly with its minimum in January or February (dry season) while the maximum is in July or August (wet season) [35]. The annual mean suspended sediment load from the Yangtze River approaches 480 million tons [36]. It has been estimated that 40% of the sediment load is deposited in the Yangtze River estuary [37]. The sediments are mainly composed of fine sand, silt and clay in the Yangtze River estuary [38]. Hydrographic conditions in the Yangtze River estuary are governed by a southward current of relatively cold and brackish water known as the Jiangsu Coastal Current in the north and the Zhejiang-Fujian Coastal Current in the south. Generally, a strong northeast winter monsoon prevails from late September to early April, and a weaker southwest summer monsoon occurs from May to August [39].

The Yangtze estuary is a mesotidal estuary with a water depth varying from 4.9 to 24 m. There exist regular semi-diurnal tides out of the mouth, and non-regular semi-diurnal tides inside, and the mean tidal range for years at Zhongjun Station nearby the mouth is 2.66 m, and a tidal flow velocity of approximately 1 m/s [37], and the tide plays a very important role which influences mass transport of the runoff into the estuary [40].

2.2. Riverbed Measurements

The bedforms of the South and North Channel, South and North Passage, Yuanyuansha waterway and the Hengsha passage in the Yangtze estuary were observed by using a Reson Seabat7125 MBES (Teledyne Technologies Inc, Thousand Oaks, CA, USA) during December 2012, February 2014, and February 2015 (Figure 2), and the surface sediment samples were collected by the grab bucket. The working frequency of the MBES can be either 200 kHz or 400 kHz. With 400 kHz, the central beam angle is 0.5° , and the beam width of launch is $1^\circ (\pm 0.2^\circ)$; the maximum ping is 50 ± 1 Hz with 512 beams; and the maximum depth resolution is 6 mm. Thus, the 400 kHz was used for the Seabat7125, with the transducer fixed on the left side of the surveying ship by cables and a custom-made shelf. The boat velocity was controlled to be as constant as possible at 2.5 m/s, and the ping was 20 Hz. The water depth of the survey site was about 20 m; thus, the maximum grid resolution was 0.3 m. Weather conditions were good during the survey period.

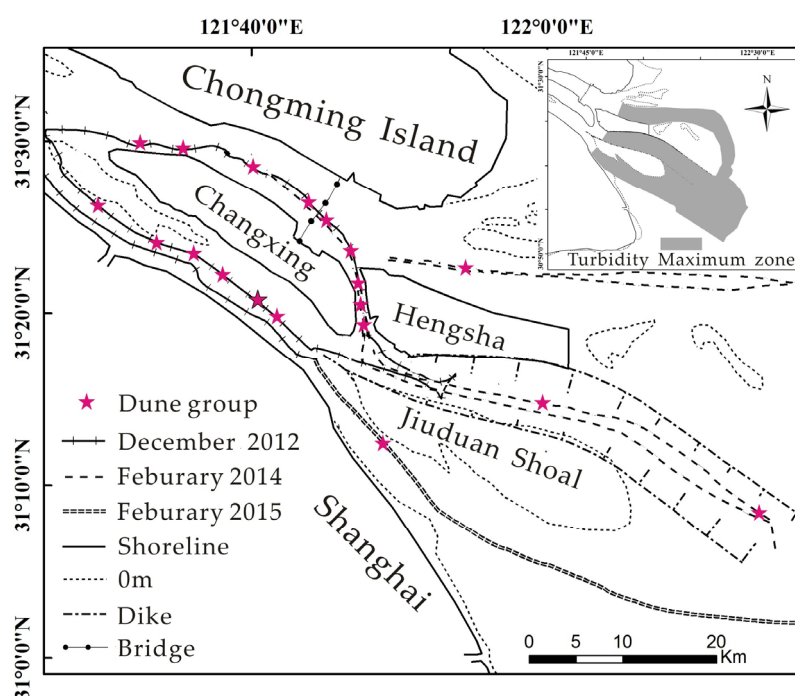


Figure 2. Field measurement routes and locations of the turbidity maximum zone in the Yangtze River estuary, China.

2.3. Field Sampling

A total of 169 sea-bottom surface sediment samples (about 2 cm) were collected from the Yangtze River estuary between 2012 and 2015 using a grab (clamshell) sampler. Grain size of the samples was analyzed using a Mastersizer 2000 Laser Granulometer (Malvern Instruments Limited, Malvern, Worcestershire, UK). Sodium phosphate (Na_2PO_3)₆ were used to disperse the samples; organic matter and CaCO_3 in the samples were removed by using 10% H_2O_2 and 10% HCL. The grain size of the samples was divided into clay (0.0005–0.004 mm), silt (0.004–0.0625 mm), and sand (0.0625–2 mm) [41].

2.4. Data Analysis

The final multi-beam data were processed by draft correction and sound speed correction. Furthermore, calibrations of roll, pitch, and yaw were conducted. The abnormal beam was removed in the editing module by using PDS2000 software (Teledyne Technologies Inc, Thousand Oaks, CA, USA). The tidal correction using the date of Wusong tide station and the base level were calibrated to the mean sea level; the altitude datum of the Wusong tide station level is 202 cm lower than mean sea level. By using a Trimble real-time differential global positioning system (DGPS), the accuracy was at the decimeter scale. In order to investigate the morphological changes in the North Channel and South Passage, we collected Admiralty charts (1:25,000 scales) of 2002, 2007, and 2013 for the study area from the Maritime Safety Administration of the People's Republic of China. These charts are government official documents that have been used in many scientific studies conducted in the lower Yangtze River estuary (e.g., [42–44]). In our study we digitized and analyzed the charts with Digital Elevation Model using ArcGIS software (ESRI, Redlands, CA, USA). Each dataset was interpolated to a grid with 200×200 m cells using the kriging interpolation technique on the ArcGIS 9.3 platform, which is widely used in morphological change analysis on the basis of bathymetric data [45–47]. The long-term discharge and sediment load data between 2002 and 2013 were collected from the Yangtze River Sediment Bulletin.

3. Results

3.1. Channel-Bed Morphology Analysis

Riverbed feature surveys during fair weather conditions showed the occurrence of wide range of sizes of dunes in the Yangtze River estuary. Overall, with the dunes being 0.12 to 3.12 m high and possessing a range of wavelength from 2.83–127.89 m, yielding a range in height to wavelength of 0.003–0.136. The vast majority of the dunes are highly asymmetric, with leeside slope angles typically between 1.57° and 29.0° , and windward slope angles typically between 1.10° and 15.51° . According to the classification scheme of Ashley [1], four classes of dunes are occurred in the Yangtze River estuary. Among all the observed dunes (1575), which very large dunes (>100 m in length) only amount to 0.3%, large dunes (10–100 m in length) predominantly occurred and amount to 51.5%, medium dunes (5–10 m in length) constitute 43.9%, and small dunes (0.6–5 m in length) represent 4.3%.

There is a large area of dunes developed in the middle and upper reaches of the Yangtze River estuary. With the dunes in the upper and middle reaches of South Channel being between 0.12 to 3.12 m in height (Table 1), and possessing a range of wavelengths from 2.83–127.89 m, respectively, the mean ratio of height to length is 0.06, among which asymmetric dunes predominantly occurred, with leeside slope angles typically between 2.20° and 29.0° , and windward slope angles typically between 1.30° and 13.78° . While the dunes in the upper and middle reaches of North Channel have heights and lengths of 0.13–2.4 m and 4.3–106.72 m, respectively, the mean ratio of height to length is 0.047, among which asymmetric dunes predominantly occurred, with leeside slope angles typically between 1.57° and 20.6° , and windward slope angles are much shallower, typically ranging from 1.10° to 9.05° .

There is also a large area of dunes developed in the Hengsha Passage. The dunes in the passage showed a wide range of heights (0.13–1.18 m) and lengths (3.74–20 m), with an average height of 0.49 m, an average length of 8.93 m, and an average height to length ratio of 0.056.

It is notable that dunes are observed for the first time in the turbidity maximum zone of the Yangtze River estuary (Figure 3). There is a small range of dunes developed in the mouth bar area of the North Channel, the middle and lower reaches of the North Passage and the south side of Jiangyanansha of the upper reach of the South Passage, respectively. Two classes of dunes occurred in the turbidity maximum zone. Among all the observed dunes (215), which large dunes predominantly occurred and amount to 69.77%, the medium dunes constitute 30.23%. The dune lies in the range of $31^\circ 22' 42.34''$ N, $121^\circ 55' 10.22''$ E to $31^\circ 22' 44.22''$ N, $121^\circ 55' 49.11''$ E; $31^\circ 14' 21.94''$ N, $122^\circ 00' 33.95''$ E

to 31°14'18.05" N, 122°01'02.23" E, and 31°07'09.10" N, 122°15'30.59" E to 31°06'59.74" N, 121°15'30.01" E, and 31°12'29.75" N, 121°49'11.99" E to 31°12'06.60" N, 121°49'40.10" E, respectively. Dune geometry is summarized in Table 2.

Table 1. Characteristics of dunes in the middle and upper reaches, and the turbidity maximum zone of the Yangtze River estuary.

Region	Height (m)		Length (m)		Windward Side Angle (°)		Lee Side Angle (°)	
	Max.	Mean	Max.	Mean	Max.	Mean	Max.	Mean
Upper and middle reaches of the SC	3.12	0.89	127.89	19.3	13.78	5.74	29.0	9.02
Upper and middle reaches of the NC	2.4	1.11	106.72	25.5	9.05	4.40	20.6	7.47
Mouth bar of the NC	1.84	0.72	95.18	15.43	12.16	5.14	19.65	9.84
Middle reach of the NP	0.74	0.48	94.27	39.41	3.49	1.65	4.19	1.81
Lower reach of the NP	0.53	0.33	14.56	11.11	15.51	5.85	4.34	2.85
Upper reach of the SP	0.57	0.35	20.07	14.83	3.50	1.82	7.42	3.40

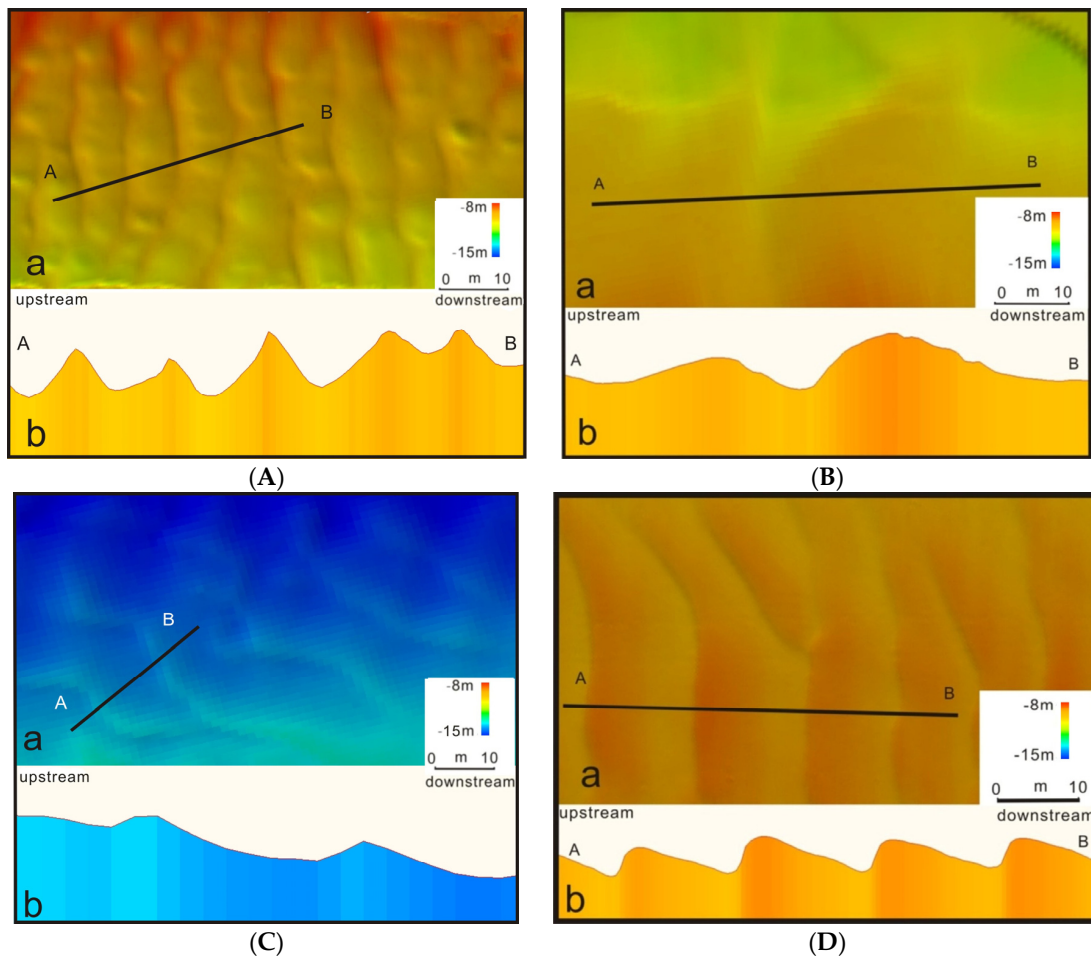


Figure 3. Subaqueous dunes in the turbidity maximum zone of the Yangtze River estuary, including (A) the dunes in the mouth bar area of the North Channel; (B) the dunes in the middle reach of the North Passage; (C) the dunes in the lower reach of the North Passage; and (D) the dunes in the south side of Jiangyanansa of the upper reach of the South Passage.

Table 2. Types and grain size distribution of sea-bottom sediment in the Yangtze estuary.

Reach	Main Type	Medium Size (Micrometer)	Content of Fine Sand (%)	Content of Silt (%)	Content of Clay (%)
Middle and upper reaches of the South Channel	Fine sand	130–178	>73	4–18	<8
Lower reach of the South Channel	Silty sand	94–123	60–65	30–35	<6
	Sandy silt	45–56	22–39	52–71	8
Yuanyuansha waterway	silt	37–51	13–18	68–74	13–18
	Sandy sit	23–72	32–38	47–55	<18
Hengsha Passage	Fine sand	130–200	>80	10–16	<4
Upper reach of the North Passage	Clayey silt	17–23	3–10	66–72	20–27
Middle reach of the North Passage	Clayey silt	10–24	2–4	64–72	24–34
Lower reach of the North Passage	silt	10–20	<5	64–70	26–36
Upper reach of the South Passage	Fine sand	136–204	>95	1–4	<1
Middle and lower reaches of the South Passage	Clayey silt	6–13	<1	55–60	37–43
Upper and middle reaches of the North Channel	Fine sand	105–237	>80	10	<6
	Silty sand	61–201	48–76	20–45	<12
Mouth bar of the North Channel	silt	15–30	10–20	65–75	10–20
	Clayey silt	7–18	2–15	60–70	20–30

3.2. Types and Grain Size of Sediment

Comparative analysis of the medium size of sea-bottom sediment of synchronous acquisition for go to survey of the Yangtze River estuary in recent years, as the results show (Figure 4, Table 2): the sea-bottom sediments distributed in Yangtze River estuary is mainly composed of fine sand, silty sand, sandy silt, silt, and clayey silt.

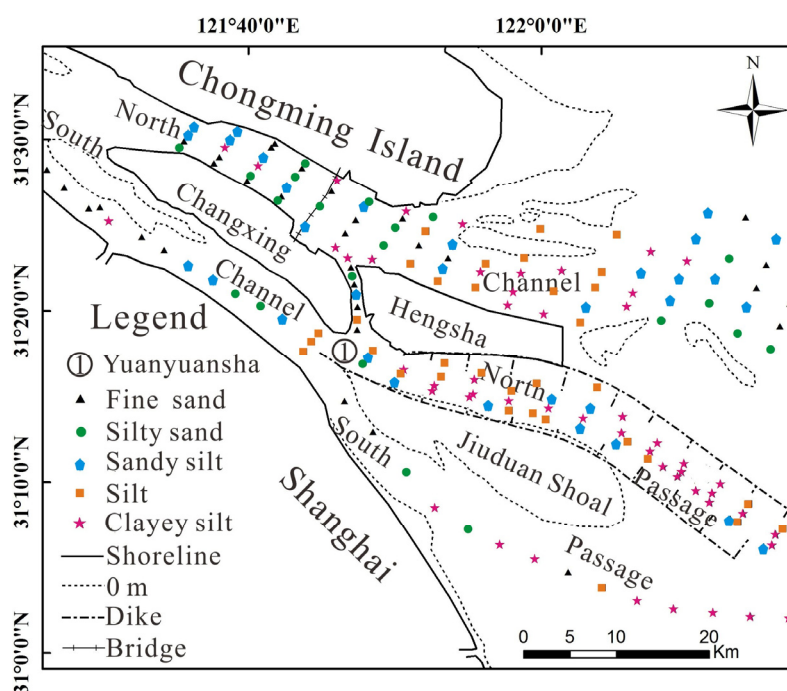


Figure 4. Types of sea-bottom sediment in the Yangtze River estuary in the recent years.

Clayey silt is the dominant sediment type (30% of all 169 sea-bottom sediment samples) and is primarily deposited in the lower reaches of the Yangtze River estuary (turbidity maximum zone), including the North Passage (14%), middle, and lower reaches of the South Passage (5%) and the mouth bar area of the North Channel (8%). Fine sand (20%) is present in the middle and upper reaches of the Yangtze River estuary, Hengsha Passage, and the primary channels of the turbidity maximum

zone, with the medium size in the range of 130–178 micrometers and 105–237 micrometers in the middle and upper reaches of the South and North Channels, 130–200 micrometers in the Hengsha Passage, 136–204 micrometer in the upper reach of the South Passage, 120–175 micrometers in the mouth bars area of the North Channel, and 144–165 micrometers in the local area of the North Passage, respectively. Silty sand (11%) is primarily present in the North Channel. Sandy silt (19%) and silt (20%) are primarily present in the estuarine mouth bar area and the Yuanyuan waterway.

4. Discussion

4.1. Factors Influencing Dune Formation in the Yangtze River Estuary

Development of dunes is related to several factors including flow conditions, sediment supply, and bed materials. Dunes are generally formed in the sandy deposit zone where mean grain size of sediments is greater than 0.125 mm [28]. However, the sea-bottom sediments distributed in the most regions of the Yangtze River estuary is mainly clayey silt, silt, and sandy silt in recent years, so the smooth surface is very common in the Yangtze River estuary. The main sea-bottom sediment distributed in the middle and upper reaches of the South and North Channels, Hengsha Passage, the upper reaches of the South Passage, the local area of the North Passage, and the local area of the mouth bars area of the North Channel is fine sand, which is one of the influence factors for the dunes developed in the above areas. Sufficient sediments are the foundation for the development of dunes [48]. Total sediment discharge amounts to approximately 5×10^{11} kg annually, and about 0.8×10^{11} kg of coarser grain-size sediment is annually deposited within the estuarine zone [28], which provides a rich source of sediments for development of dune.

Previous studies have shown that bed material was composed of silt and clay in the turbidity maximum zone of the Yangtze River estuary [49]. Recent studies also suggested that the main sediment distributed in the South Passage and North Passage in recent years was clayey silt and there were no dunes during any of the measurements [27,50]. However, the results in this paper indicate that the main sediment distributed in the upper reach of the South Passage, the local area of the middle and lower reaches of the North Passage, and the local area of the mouth bar area of the North Channel is fine sand. Moreover, a small area of dunes has developed in the above areas, and the dunes are observed for the first time in the turbidity maximum zone of the Yangtze estuary.

The reasons why the dunes developed in the turbidity maximum zone may be related to the declining riverine sediment supply and estuarine engineering. Due to the sediment discharge from the Yangtze drainage basin rapidly decreasing and the implementation of the large-scale estuarine engineering within the North Channel, especially the construction of the Qingcaosha reservoir project in June of 2007, there was significant erosion in the middle and upper reaches of the North Channel [51], and local erosion occurred in the mouth bar area of North Channel (Figure 5), resulting in a significant coarsening of the bed material in the area. Coarse sands can build dunes more easily than fine sands under the same flow conditions [52]. The dunes developed in the South Passage and North Passage were closely related to the Deepening Waterway Project. Due to the construction of two training walls and ten groins within the North Passage, the ebb flow diversion ratio of the North Passage and the South Passage changed significantly and the ebb flow diversion ratio of the South Passage increased significantly [42]. Consequently, the upper reach of the South Passage experienced significant erosion (Figure 6), resulting in a significant coarsening of the bed material in the area, which may have contributed to the development of dunes in the upper reach of the South Passage. The hydrodynamic of the local area of the North Passage changed obviously because of the dredging project [42], which may be associated with the development of dunes in the local area of the middle and lower reaches of the North Passage.

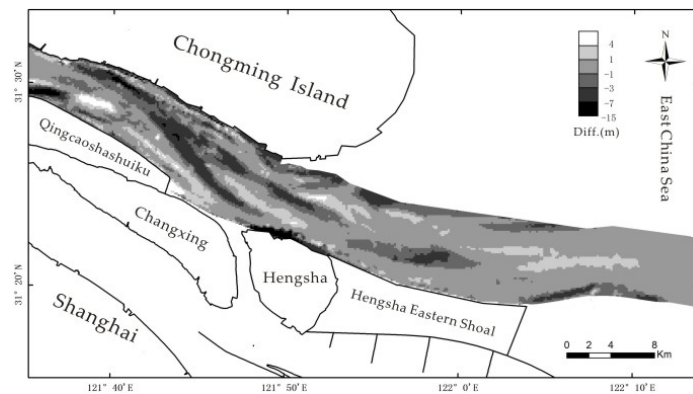


Figure 5. Thickness of deposition or erosion in the North Channel from 2007 to 2013 (negative values indicate net erosion; while positive values indicate net accretion).

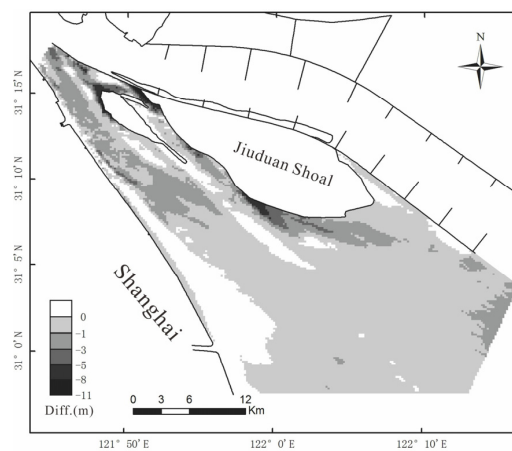


Figure 6. Thickness of deposition or erosion in the South Passage from 2002 to 2013 (negative values indicate net erosion; while positive values indicate net accretion).

4.2. Factors Influencing and Denotative of Dune Geometry

Scale of dunes are dependent on the river discharge, with large dunes occurring in the high-discharge regime, and medium dunes occurring in the low-discharge regime in the Yangtze River estuary [28]. The ebb-flow diversion ratio of the North Channel is larger than the South Channel in the recent years [53], while the water and sediment discharge of the Hengsha Passage is lesser. Consequently, much larger dunes (an average height of 1.11 m and an average length of 25.5 m) were detected in the upper and middle reaches of North Channel, many small dunes (an average height of 0.89 m and an average length of 19.3 m) occurred in the upper and middle reaches of the South Channel, while even smaller dunes (an average height of 0.49 m and an average length of 8.93 m) were measured in the Hengsha Passage. The ebb-flow diversion ratio of the North Passage and the South Passage changed significantly and the ebb-flow diversion ratio of the South Passage increased significantly in recent years [42], while river discharge of the South Passage and North Passage originated from the South Channel, which is smaller than the mouth bar area of the North Channel [53]. Consequently, much larger dunes (an average height of 0.72 m and an average length of 15.43 m) were detected in the mouth bar area of the North Channel, many small dunes (an average height of 0.35 m and an average length of 14.83 m) occurred in the upper reach of the South Passage, while even smaller dunes (an average height of 0.33 m and an average length of 11.11 m) were measured in the lower reach of North Passage, but the dunes scale (an average height of 0.48 m and an average length of 39.41 m) is larger in the middle reach of the North Passage, which may be related to the back silting mainly concentrated in the middle reach of the North Passage [54].

The mean ratio of dune height to dune length is 0.06 and 0.047 for the upper and middle reaches of the South Channel and North Channel, respectively, and 0.056 for the Hengsha Passage, indicating that there is little difference in the geometry of these dunes. The mean leeside slope angle of the dunes in the channels (9.02° , 7.47° , 9.84° , 3.40° , and 1.81°) is significantly larger than the mean windward slope angles of dunes (5.74° , 4.40° , 5.14° , 1.82° , and 1.65°) in the upper and middle reaches of the South Channel and North Channel, the mouth bar area of the North Channel, the upper reach of the South Passage, and the middle reach of the North Passage, respectively. The results suggest that the steep slopes of asymmetrical dunes in the middle and upper reaches, and the turbidity maximum zone of the Yangtze River estuary face predominantly towards tides because of the ebb-dominated currents [28]. While the mean leeside slope angles of 2.85° is significantly smaller than the mean windward slope angles of 5.85° in the lower reach of North Passage, indicating the steep slopes of asymmetrical dunes face upstream because of the flood-dominated currents. In addition, the leeside slope angles have low angles of (3.40° , 1.81° , and 2.85°) in the upper reach of the South Passage and the middle and lower reaches of the North Passage, which may be related to deposition of suspended sediment in the dune troughs [55].

The factors that have significant influences on the morphological change of dunes are flow regime, channel pattern, and bed materials. In the past years, discharge of the Yangtze River estuary and the channel pattern of the South Channel have not changed much (Figure 7). Therefore, the morphological change of dunes could be mainly attributed to the change in sediment supply in the South Channel. During 2002 and 2013, sediment discharge at the Datong station fluctuated greatly with a declining trend, which may have contributed to bed erosion of the bifurcation of the North and South Channel [27]. The erosion of the shoals has led to a large quantity of coarser sediments being transported into the South Channel, resulting in the growth of the dunes and the seaward of the dune zone and in the South Channel [27]. Consequently, it is likely that the scale of dunes will increase in the future. For example, much larger dunes with an average length of 19.3 m were detected in the South Channel during the dry season in December 2012, much small dunes with an average length of 14.1 m occurred in the South Channel during the dry season in February 2006, while even smaller dunes with an average length of 13.7 m were measured in the South Channel during the dry season in December 1997 (Table 3).

Table 3. Statistical characteristic of dunes in the South Channel of the Yangtze River estuary.

Dune regime	Height (m)		Length (m)		Windward Side Angle ($^\circ$)		Lee Side Angle ($^\circ$)	
	Max.	Mean	Max.	Mean	Max.	Mean	Max.	Mean
South Channel(1997.12) [28]	1.3	0.5	51.6	13.7	7.5	3.8	11.8	5.6
South Channel(2006.2) [27]	1.4	0.6	55.7	14.1	6.5	3.2	11.0	5.0
South Channel(2012.12)	3.12	0.89	127.89	19.3	13.78	5.74	29	9.02

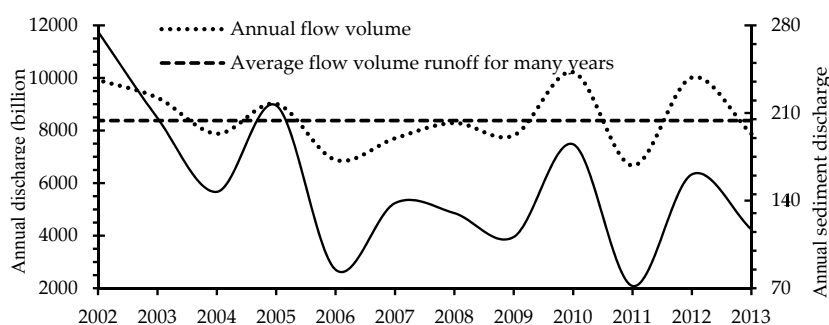


Figure 7. Change of the annual flow volume and suspended sediment yield in recent years at the Datong station on the Yangtze River estuary.

5. Conclusions

This study analyzed the recent development and characteristics of riverbed micromorphology of the Yangtze River estuary. The findings show that a large area in the middle and upper reaches of the estuary riverbed has developed dunes, indicating that dunes were well developed in channels where sands were the dominant component of bed material. A small area of dunes was observed for the first time in the turbidity maximum zone of the Yangtze River estuary, which may have resulted from a declining riverine sediment supply and estuarine engineering. Large dunes were found predominant, amounting to 51.5%, which could possess serious safety risks in estuarine engineering, pipeline construction, and sailing. These large dunes may also have the potential to decrease navigable depths, thus making frequent dredging activities necessary and increasing dredging costs. It is likely that the scale of these dunes will increase in the future in the South Channel due to a sharp decline of sediment discharge caused by the recent human activities in the upper river reach. There is a need to further investigate the origin and characteristics of subaqueous dunes in the Yangtze River estuary, and determine how micromorphology of the estuarine bed is affected by upstream river engineering.

Acknowledgments: This study was financially supported by the Natural Science Foundation of China (Grant Number: 41476075).

Author Contributions: Shuaihu Wu carried out multi-beam bathymetric data analyses, and wrote the first manuscript draft. Heqin Cheng provided the bathymetric data and Jiufa Li provided the sea-bottom sediment data. Shuaihu Wu, Heqin Cheng and Y. Jun Xu developed the study concept. Y. Jun Xu provided suggestions on the data analysis and manuscript preparation, and revised the manuscript at all stages. All authors read and approved the final manuscript.

Conflicts of Interest: The authors declare no conflict of interest.

References

1. Ashley, G.M. Classification of large-scale subaqueous bed forms: A new look at an old problem. *J. Sediment. Res.* **1990**, *1*, 160–172.
2. Dalrymple, R.W.; Hoogendoorn, E.L. Erosion and deposition on migrating shoreface-attached ridges, Sable Island, Eastern Canada. *Geosci. Can.* **1997**, *24*, 350–360.
3. Knaapen, M.A.F.; Hulscher, S.J.M.H.; Vriend, H.J.; Stolk, A. A new type of sea bed waves. *Geophys. Res. Lett.* **2001**, *28*, 1323–1326. [[CrossRef](#)]
4. Kostaschuk, R. A field study of turbulence and sediment dynamics over subaqueous dunes with flow separation. *Sedimentology* **2000**, *47*, 519–531. [[CrossRef](#)]
5. Warmink, J.J.; Dohmen-Janssen, C.M.; Lansink, J.; Naqshband, S.; van Duin, O.J.M.; Paarlberg, A.J.; Termes, P.; Hulscher, S.J.M.H. Understanding river dune splitting through flume experiments and analysis of a dune evolution model. *Earth Surf. Process. Landf.* **2014**, *39*, 1208–1220. [[CrossRef](#)]
6. Baas, J.H. A flume study on the development and equilibrium morphology of current ripples in very fine sand. *Sedimentology* **1994**, *41*, 185–209. [[CrossRef](#)]
7. Van Rijn, L.C. Sediment transport part III: bedforms and alluvial roughness. *J. Hydraul. Eng. ASCE.* **1984**, *110*, 1733–1754. [[CrossRef](#)]
8. Parsons, D.R.; Best, J.L.; Orfeo, O.; Hardy, R.J.; Kostaschuk, R.; Lane, S.N. Morphology and flow fields of three-dimensional dunes, Rio Parana, Argentina: Results from simultaneous multibeam echo sounding and acoustic Doppler current profiling. *J. Geophys. Res.* **2005**, *110*, 1–9. [[CrossRef](#)]
9. Mclean, S.R.; Nelson, J.M.; Wolfe, S.R. Turbulence structure over two-dimensional bedforms: Implications for sediment transport. *J. Geophys. Res.* **1994**, *99*, 12729–12747. [[CrossRef](#)]
10. Nelson, J.M.; Wolfe, S.R. Mean flow and turbulence over two-dimensional bedforms. *Water Resour. Res.* **1993**, *29*, 3935–3953. [[CrossRef](#)]
11. Amsler, M.L.; Garcia, M.H. Sand dune geometry of large rivers during floods: Discussion. *J. Hydraul. Eng.* **1997**, *123*, 582–584. [[CrossRef](#)]
12. ASCE Task Force. Flow and transport over dunes. *J. Hydraul. Eng.* **2002**, *127*, 726–728.
13. Best, J. The fluid dynamics of river dunes: A review and some future research directions. *J. Geophys. Res.* **2005**, *110*, 1–21. [[CrossRef](#)]

14. Nemeth, A.; Hulscher, S.; Van Damme, R.M.J. Simulating offshore sand waves. *Coast. Eng.* **2006**, *53*, 265–275. [[CrossRef](#)]
15. Nemeth, A.; Hulscher, S.; de Vriend, H.J. Modeling sand wave migration in shallow shelf seas. *Cont. Shelf Res.* **2002**, *22*, 2795–2806. [[CrossRef](#)]
16. Morelissen, R.; Hulscher, S.J.M.H.; Knaapen, M.A.F.; Nemeth, A.; Bijker, R. Mathematical modeling of sandwave migration and the interaction with pipelines. *Coast. Eng.* **2003**, *48*, 197–209. [[CrossRef](#)]
17. Catano-Lopera, Y.A.; Abad, J.D.; Garcia, M.H. Characterization of bedform morphology generated under combined flows and currents using wavelet analysis. *Ocean Eng.* **2009**, *36*, 617–632. [[CrossRef](#)]
18. Besio, G.; Blondeaux, P.; Brocchini, M.; Hulscher, S.J.M.H.; Idier, D.; Knaapen, M.A.F.; Ne'meth, A.A.; Roos, P.C.; Vittori, G. The morphodynamics of tidal sand waves: A model overview. *Coast. Eng.* **2008**, *55*, 657–670. [[CrossRef](#)]
19. Ashworth, P.J.; Best, J.L.; Roden, J.E.; Bristow, C.S.; Klaassen, G.J. Morphological evolution and dynamics of a large, sand braid-bar, Jamuna River, Bangladesh. *Sedimentology* **2000**, *47*, 533–555. [[CrossRef](#)]
20. Karim, F. Bed-form geometry in sand-bed flows. *J. Hydraul. Eng. ASCE* **1999**, *125*, 1253–1261. [[CrossRef](#)]
21. Perillo, M.M.; Best, J.L.; Yokokawa, M.; Sekiguchi, T.; Takagawa, T.; Garcia, M.H. A unified model for bedform development and equilibrium under unidirectional, oscillatory and combined-flows. *Sedimentology* **2014**, *61*, 2063–2085. [[CrossRef](#)]
22. Van Landeghem, K.J.J.; Wheeler, A.J.; Mitchell, N.C.; Sutton, G.D. Variations in sediment wave dimensions across the tidally dominated Irish Sea, NW Europe. *Mar. Geol.* **2009**, *263*, 108–119. [[CrossRef](#)]
23. Van der Veen, H.H.; Hulscher, S.J.M.H.; Knaapen, M.A.F. Grain size dependency in the occurrence of sand waves. *Ocean Dyn.* **2006**, *56*, 228–234. [[CrossRef](#)]
24. Knaapen, M.A.F. Sandwave migration predictor based on shape information. *J. Geophys. Res.* **2005**, *110*, 312–321. [[CrossRef](#)]
25. Hernandez-Azcunaga, L.; Carbajal, N.; Montano-Ley, Y. Bed load transport of sediments and morphodynamics in the Northern gulf of California. *J. Coast. Res.* **2014**, *30*, 228–236. [[CrossRef](#)]
26. Cheng, H.Q.; Kostaschuk, R.; Shi, Z. Tidal currents, Bed Sediments, and Bedforms at the South Branch and the South Channel of the Chajiang (Yangtze) Estuary, China: Implications for the ripple-dune transition. *Estuaries* **2004**, *27*, 861–866. [[CrossRef](#)]
27. Li, W.; Cheng, H.; Li, J.; Dong, P. Temporal and spatial changes of dunes in the Changjiang (Yangtze) estuary, China. *Estuar. Coast. Shelf Sci.* **2008**, *77*, 169–174.
28. Wu, J.; Wang, Y.; Cheng, H. Bedforms and bed material transport pathways in the Changjiang (Yangtze) Estuary. *Geomorphology* **2009**, *104*, 175–184. [[CrossRef](#)]
29. Zhang, Q.; Xu, C.Y.; Singh, V.P.; Yang, T. Multiscale variability of sediment load and streamflow of the lower Yangtze River basin: Possible causes and implications. *J. Hydrol.* **2009**, *368*, 96–104. [[CrossRef](#)]
30. Luo, X.X.; Yang, S.L.; Zhang, J. The impact of Three Gorges Dam on the downstream distribution and texture of sediments along the middle and lower Yangtze River (Changjiang) and its estuary, and subsequent sediment dispersal in the East China Sea. *Geomorphology* **2012**, *179*, 126–140. [[CrossRef](#)]
31. Chen, Z.; Yu, L.; Gupta, A. The Yangtze River: An introduction. *Geomorphology* **2001**, *41*, 73–75. [[CrossRef](#)]
32. Yang, S.L.; Zhang, J.; Dai, S.B.; Li, M.; Xu, X.J. Effect of deposition and erosion within the main river channel and large lakes on sediment delivery to the estuary of the Yangtze River. *J. Geophys. Res.* **2007**, *112*. [[CrossRef](#)]
33. Chao, M.; Shi, Y.; Quan, W.; Shen, X. Distribution of Macrocrustaceans in Relation to Abiotic and Biotic Variables across the Yangtze River Estuary, China. *J. Coast. Res.* **2015**, *31*, 946–956. [[CrossRef](#)]
34. Shen, H.; Li, J.; Zhu, H.; Han, M.; Zhou, F. Transport of the suspended sediment in the Changjiang Estuary. *Int. J. Sediment Res.* **1993**, *7*, 45–63.
35. Pu, X.; Shi, J.Z.; Hu, G.; Xiong, L. Circulation and mixing along the North Passage in the Changjiang River Estuary, China. *J. Mar. Syst.* **2015**, *148*, 213–235. [[CrossRef](#)]
36. Song, D.; Wang, X.; Cao, Z.; Guan, W. Suspended sediment transport in the Deepwater Navigation Channel, Yangtze River Estuary, China, in the dry season 2009: 1. Observations over spring and neap tidal cycles. *J. Geophys. Res. Ocean.* **2013**, *118*, 5555–5567. [[CrossRef](#)]
37. Milliman, J.D.; Shen, H.; Yang, Z.; Meades, R.H. Transport and deposition of river sediment in the Changjiang estuary and adjacent continental shelf. *Cont. Shelf Res.* **1985**, *4*, 37–45. [[CrossRef](#)]
38. Liu, H.; He, Q.; Wang, Z.; Weltje, G.J.; Zhang, J. Dynamics and spatial variability of near-bottom sediment exchange in the Yangtze Estuary, China. *Estuar. Coast. Shelf Sci.* **2010**, *86*, 322–330. [[CrossRef](#)]

39. Yang, B.; Cao, L.; Liu, S.; Zhang, G. Biogeochemistry of bulk organic matter and biogenic elements in surface sediments of the Yangtze River Estuary and adjacent sea. *Mar. Pollut. Bull.* **2015**, *96*, 471–484. [[CrossRef](#)] [[PubMed](#)]
40. Wang, Y.; Shen, J.; He, Q. A numerical model study of the transport time scale and change of estuarine circulation due to waterway constructions in the Changjiang Estuary, China. *J. Mar. Syst.* **2010**, *82*, 154–170. [[CrossRef](#)]
41. Shepard, F.P. Nomenclature based on sand–silt–clay ratios. *J. Sediment. Res.* **1954**, *24*, 151–158.
42. Jiang, C.; Li, J.; de Swart, H.E. Effects of navigational works on morphological changes in the bar area of the Yangtze River Estuary. *Geomorphology* **2012**, *139*, 205–219.
43. Ji, N.; Cheng, H.; Yang, Z.; Hu, H.; Chen, Z. Sedimentary and morphological evolution of nearshore coast of Yangtze Estuary in the last 30 years. *Acta Geogr. Sin.* **2013**, *68*, 945–954. (In Chinese)
44. He, Y.; Cheng, H.; Chen, J. Morphological Evolution of Mouth Bars of the Yangtze Estuarine Waterways in the Last 100 Years. *Acta Geogr. Sin.* **2011**, *66*, 305–312. (In Chinese) [[CrossRef](#)]
45. Zhao, H.; Zhou, J.; Zhao, J. Tidal impact on the dynamic behavior of dissolved pharmaceuticals in the Yangtze Estuary, China. *Sci. Total Environ.* **2015**, *536*, 946–954. [[CrossRef](#)] [[PubMed](#)]
46. Van der Wal, D.; Pye, K.; Neal, A. Long-term morphological change in the Ribble Estuary, northwest England. *Mar. Geol.* **2002**, *189*, 249–266. [[CrossRef](#)]
47. Van der Wal, D.; Pye, K. The use of historical bathymetric charts in a GIS to assess morphological change in estuaries. *Geogr. J.* **2003**, *169*, 21–31. [[CrossRef](#)]
48. Wu, Z.Y.; Jin, X.L.; Li, J.B. Linear sand ridges on the outer shelf of the East China Sea. *China Sci. Bull.* **2005**, *50*, 2517–2528. (In Chinese) [[CrossRef](#)]
49. Li, J.; Shi, W.; Shen, H. Sediment properties and transportation in the turbidity maximum in Changjiang Estuary. *Geogr. Res.* **1994**, *13*, 51–59. (In Chinese)
50. Zhou, C.X. On sandwaves in Yawosha channel of the Yangtze Estuary. In Proceedings of the Second International Symposium on River Sedimentation, Nanjing, China, 11–16 October 1983; Water Resources and Electric Power Press: Beijing, China, 1983; pp. 650–661.
51. Liu, W.; Tang, J.; Miu, S. Study on evolution trend of North Channel of Yangtze River Estuary and influences of related projects. *Yangtze River* **2011**, *42*, 39–43. (In Chinese)
52. Southard, J.B.; Boguchwal, A.L. Bed configurations in steady unidirectional water flows. Part 2. Synthesis of flume data. *J. Sediment. Res.* **1990**, *60*, 658–679. [[CrossRef](#)]
53. Mao, Z.; Wu, X.; Zhao, C.; Guo, J. Evolution of the upper reach of mouth bars in the North Channel of the Changjiang Estuary. *J. Sediment Res.* **2008**, *2*, 41–46. (In Chinese)
54. Dai, Z.; Liu, J.T.; Fu, G.; Xie, H. A thirteen-year record of bathymetric changes in the North Passage, Changjiang (Yangtze) estuary. *Geomorphology* **2013**, *187*, 101–107. [[CrossRef](#)]
55. Kostaschuk, R.A.; Villard, P.V. Flow and sediment transport over large subaqueous dunes: Fraser River, Canada. *Sedimentology* **1996**, *43*, 849–863. [[CrossRef](#)]

